

COB-2023-0355

LEAKS IDENTIFICATION AND CLASSIFICATION FROM PRESSURE SIGNATURE IN DENSE-GAS/LIQUID PIPE FLOW

Carlos M. Ruiz-Diaz
Castro-B. Johann E.
C. E. Alvarez-Pacheco
M. da Silva Carr
Oscar M. H. Rodriguez

University of São Paulo (USP), São Carlos School of Engineering (ESSC), Mechanical Engineering Department, Industrial Multiphase Flow Laboratory (LEMI), Av. Trab. São Carlense, 400 - Parque Arnold Schimidt, São Carlos - SP, 13566-590, Brazil.
carlosruiz978@usp.br, cristhianeap@usp.br, johanncastro@usp.br, marcus_carr@usp.br, oscarmhr@sc.usp.br

Abstract. In the hydrocarbon industry, flow assurance is an important factor for the operation of oil and gas wells, which can be exposed to deviations in their normal flow conditions. This increases the cost of system maintenance and results in a considerable loss of resources, ultimately affecting the environment. Therefore, the accurate and fast detection of anomalies or deviations in pipelines is critical for the safe and profitable production and transportation of oil and gas, as it prevents unexpected failures or shutdowns in production. However, it is worth highlighting the difficulty of finding sensors installed in pipelines that can directly detect the occurrence of undesired events. When sensors are found, it is often impractical to install them. Traditional prediction and classification methods based on physical models or purely on real data collected from wells or simulated data using specialized software have limitations, such as high uncertainty and high computational cost. In this research, an experimental campaign was carried out to collect experimental data under hydrodynamically similar conditions to the Brazilian pre-salt layer, where controlled and monitored normal condition without leak-type anomalies was developed. A total of eighteen experimental data points were generated in the Industrial Multiphase Flow Laboratory - LEMI under specific conditions to investigate the behavior of two-phase dense-gas/oil flow in horizontal position. These measurements allowed for the determination of the pressure drop and void fraction associated with each flow pattern. Additionally, a reference state was established for pressure drop in a SF₆-oil horizontal pipe through global and windowed signal analysis based on pressure drop signature from a differential pressure sensor. The results show that the oscillatory process is stationary with a tendency towards a constant value that depends on the operational conditions.

Keywords: leakage, dense gas, two-phase flow, differential pressure signature

1. INTRODUCTION

In the oil and gas industry, flow assurance is an important factor for the safe operation of wells, which are constantly subjected to anomalies during their operation (Nascimento; et al., 2021), such as leaks, which can occur in production pipelines. It is worth noting the difficulty of finding line sensors capable of directly detecting leak occurrences. When found, their installation is often impractical and require an unfeasible increase in data acquisition frequency.

Failures and unexpected production interruptions in the oil and gas industry due to leaks not only increase maintenance costs but also pose environmental risks in the production area and endanger the operators. These factors justify the growing concern to improve the current systems for prediction and detection of leaks in the Brazilian pre-salt pipelines (Marins et al., 2021; Turan & Jaschke, 2021; Vargas et al., 2019). One common and significant phenomenon observed in the installed flexible lines in the Brazilian pre-salt is stress corrosion cracking (SCC-CO₂), which involves tension, corrosion, and cracks in the presence of CO₂. SCC-CO₂ is one of the leading causes of leaks in the pipelines of oil and gas extraction platforms, leading to wear and pipe fissures.

The classical approach to study leakage anomalies is based on the variation in the hydrodynamic energy curve. In this study, dynamic pressure signals will be used to detect and classify leaks with distinct labels. This is because dynamic pressure signals allow for deep analysis of the signature of the differential pressure signal. This will be achieved by applying advanced techniques such as statistical property analysis of temporal signals or using Fourier and Gabor transforms, auto-correlation and cross-correlation, relative phase estimator, among others (dos Santos Ambrosio et al., 2022; Saon Crispim Vieira et al., 2021). These and other techniques have been successfully used for the classification of two-phase flow patterns, either in a deterministic manner (Álvarez-Briceño et al., 2023) or as features for ANN and SVM classifiers in the context of machine learning (Borg et al., 2021; Sestito et al., 2022).

Detection of this anomaly depends initially on the identification of the characteristics of the normal operating condition, and subsequently, the identification of anomalous conditions through comparison with the normal condition

(Martins & Seleghim, 2010), even if data from anomalous conditions are not available a priori (Borg et al., 2021; Saon C. Vieira et al., 2023).

There are practical strategies for leak detection in pipes based on external and internal detection methods. The external methods consist of the use of sensors such as an optical fiber, acoustic systems, semi-permeable sensors, and video monitoring. The internal methods are based on pressure point monitoring and analysis, mass balance method, statistical methods and real time transient model (RTTM) (Fiedler, 2016; Idachaba & Tomomewo, 2023). In real systems, the internal and external methods are commonly used together to take advantage of each method's advantages.

The internal methods have been evaluated based on a few parameters: the minimum detectable rate, time to detect leaks in pipes, type of the leaks, and the false alarm rate. This information is summarized in Table 1 (Blázquez-García et al., 2021; Shao et al., 2019).

Although the mass balance and statistical methods are capable of detecting low leakage rates and spontaneous and creeping leaks, the time it takes to detect them is very high. This is a crucial variable, as the fluids can cause damage to the environment if they are not detected and repaired quickly. Consequently, the pressure point and RTTM methods are shown to be superior due to their fast response time. These methods may, however, provide false alarms depending on the flow pattern and the external conditions of the pipes (Idachaba & Tomomewo, 2023).

Table 1. Methods for leak detection in pipes. Adapted from (Fiedler, 2016)

Method	Min rate	Time to detect	Type of leaks	False alarm
Mass Balance	1%	Long	Spontaneous	High
RTTM	1%	Short	Spontaneous and creeping	Average
Statistical	0.5%	Long	Spontaneous and creeping	slight
Pressure point analysis	5%	Short	Spontaneous	High

These methods do not consider the correlation over time of data collected by different sensors or time windows within the analyzed time series (Blázquez-García et al., 2021). Keeping this in mind, this work presents a time windowed analysis based on the average, variance, and autocorrelation of the signals. Such method is typically used in signal processing and classification of the time series in stationary and non-stationary processes (Moretin & Toloï, 2006). This methodology aims to provide a reference state for classification of pressure time-series collected for oil-SF₆ horizontal pipes and, to be later extended to oil-SF₆ with leaks under different operational conditions.

2. METHODOLOGY

The methodology was developed considering the devices installed in the new experimental apparatus of the Industrial Multiphase Flow Laboratory (LEMI) at the University of São Paulo on the São Carlos campus.

2.1 Experimental apparatus

The experimental apparatus employed in this study consists of a 30 meter long U-shaped pipe capable of working with two-phase flow, which is subdivided into two 15 meter sections, one upstream and one downstream that goes directly to the separator tanks. A separate 0.0254 meter (i.d.) pipe for the leak outlet is installed too. The apparatus includes a test section equipped with a visualization window, a high-speed camera, pressure, temperature, and flowmeter sensors, and pneumatically controlled quick-closing directional valves. More detailed specifications of the apparatus can be found in Table 2

Table 2. Experimental apparatus capabilities.

Parameter	Measurement	Units
Inclination	- 90 to 90	deg
Internal diameter	50.8	mm
L/d	237 – 355	-
Max. Oil Volumetric flow rate	40	m ³ /h
Max. SF ₆ Volumetric flow rate	3062	kg/h
Temperature range	15 – 50	°C
Absolute inner pressure	15	bar
Density ratio	~10	-

To generate novel insights, we developed a unique methodology that utilizes dense-gas and mineral oil as working fluids under specific pressure and temperature conditions. A schematic representation of the installation is presented in Figure 1, referring to the high-pressure line installed.

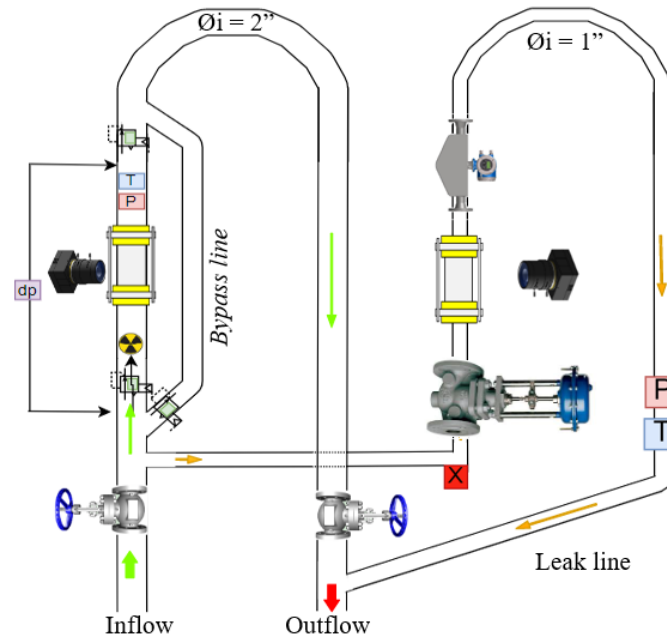


Figure 1. Schematic representation of the experimental loop with the new leak line.

The apparatus can operate with inclinations ranging from 0 to 90 degrees, allowing for the study of flows in both upward and downward inclinations. The LEMI represents a unique facility in Brazil and stands out globally due to its capability to acquire experimental data under hydrodynamic conditions that closely resemble those encountered in deepwater pre-salt production operations. The distinguishing feature of LEMI lies in its utilization of dense-gas within the high-pressure line, enabling the investigation of liquid-gas density ratios below 10, a parameter highly representative of the prevailing conditions in the pre-salt reservoirs.

The properties of the substances utilized are presented in Table 3.

Table 3. Physical properties of the fluids used at 15 bar and 25°C.

Phase	Fluid	Density [kg/m ³]	Viscosity [cP]
Oil	Turbine 22	867.1	22
Dense - gas	SF ₆	110.1	0.015

Taking into account the operational capability of the tilting platform of LEMI, an experimental campaign was meticulously devised with the platform positioned horizontally. Consequently, a set of 18 distinct experimental conditions were developed, with the explicit purpose of generating fresh insights into the realm of dense-gas and oil two-phase flow. This endeavor serves as a valuable complement to the comprehensive research conducted by (Quintino, 2022), which was centered around the normal condition devoid of any leakage through the 0.0508 m i.d. pipe. It is important to note that said pipeline was subjected to an approximate pressure of 14 bar. The experimental matrix is presented in Figure 2, where the superficial velocities of the fluids are located on the vertical and horizontal axes. U_{SL} represents the superficial velocity of the liquid, while U_{SG} represents the superficial velocity of the gas.

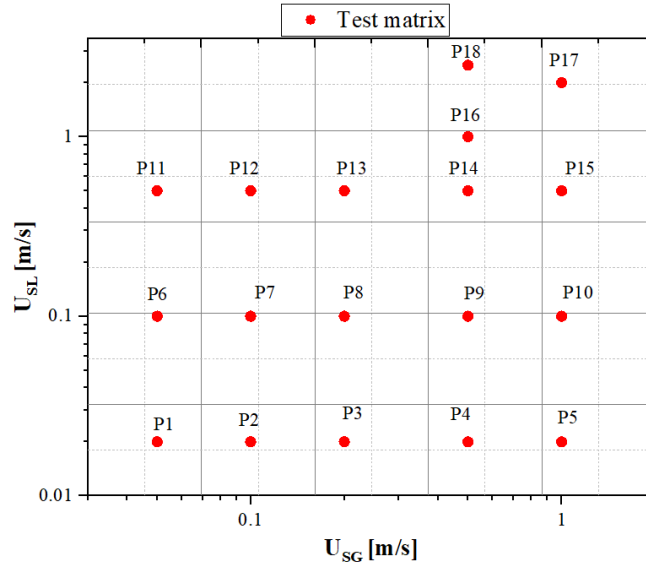


Figure 2. Experimental matrix.

2.2 Signal processing

To accurately measure the pressure difference between two points within the test section, a high-precision differential pressure sensor was installed. This advanced sensor was capable of capturing pressure differentials ranging from -3 kPa to 3 kPa, with the pressure taps strategically positioned 1.7 meters apart.

Assuming that the signal collected by the differential pressure sensor in the presence of background noise are of the form:

$$x(n) = s(n) + N(n) \quad (1)$$

where $x(n)$, $s(n)$ and $N(n)$ correspond to the time series acquired by the data acquisition system, the signal from differential pressure sensor and the background noise, respectively.

Based on this model, the time series $x(t)$, given by the differential pressure sensor corresponds to a set of observations ordered in time, in this case, equally spaced by a quantity $\Delta=1/f_s$ (Moretin & Toloï, 2006). Where f_s corresponds to a sampling frequency of the DP sensor. Typically, the characterization of a time-series is based on its stationarity of the process. This means that the data vary around a constant mean and remain independent of time. Additionally, the variance of the data should remain constant over time (Moretin & Toloï, 2006; Shao et al., 2019). The average value μ , the variance $\text{Var}(x)$ and the autocorrelation $R_{xx}(\tau)$ function is given in equations (2),

(3) and (4), respectively:

$$\mu = \frac{1}{n} \sum_{i=1}^n x(n\Delta) \quad (2)$$

$$\text{Var}(x) = \sigma^2 = \frac{1}{n} \sum_{i=1}^n (x(n\Delta) - \mu)^2 \quad (3)$$

$$R_{xx}(\tau) = \frac{\sum_{i=1}^n [x(n\Delta) - \mu][x(n\Delta + \tau) - \mu]}{\sum_{i=1}^n [x(n\Delta) - \mu]^2} \quad (4)$$

The autocorrelation function defines the relation between the actual observations and the later observations, i.e., that its own values are directly related with their precedent values (Shin & Hammond, 2008).

For a stationary process, the signal $x(n)$ should has a mean $\mu = 0$, the variance σ^2 must be constant and the autocorrelation function must be decrease rapidly to zero (Morettin, 2006). These hypotheses will be verified for the overall signal, and, for a decomposition of each time series into an equally spaced sub-intervals of time, as shown in Figure 3. It is important to note that a moving mean filter was used to eliminate the noise present in the signal before the

time-series analysis. Finally, if the signal satisfies those conditions, it will be considered stationary and can be used to predict the pressure drop in oil-SF₆ horizontal pipe flows using predictive models, such as ARIMA or Box Jenkins.

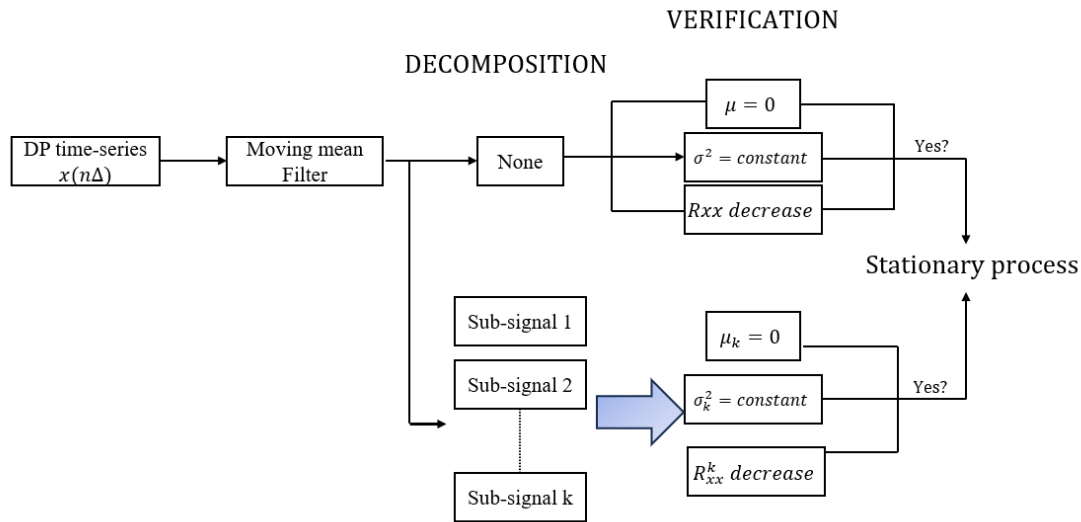


Figure 3. Algorithm Verification for the DP time-series used in this study.

3. RESULTS AND DISCUSSION

The proposed experimental campaign with the 18 conditions was conducted, where the maximum velocity achieved by the gas was 1 m/s and that of the oil was 2 m/s. In the experimental development, the main challenge was to achieve a gas density of approximately 100 kg/m³ in order to obtain a density ratio between 8 and 10.

The visualized flow patterns included smooth stratified flow (Figure 4), wavy stratified flow (Figure 5), stratified flow with dispersion, and gas bubble dispersion in the liquid phase. The flow propagated from left to right. All experimental data points were characterized based on the determination of the holdup, pressure gradient, and flow pattern classification.

To determine the volumetric liquid fraction, a cesium-137 gamma densitometer emitting a maximum energy of 660 keV was used. It was installed on a vertical displacement system, allowing cordal measurements across the cross-section of the pipe.



Figure 4. Smooth stratified flow pattern observed ($U_{sl} = 0.02$ m/s, $U_{sg} = 0.1$ m/s).

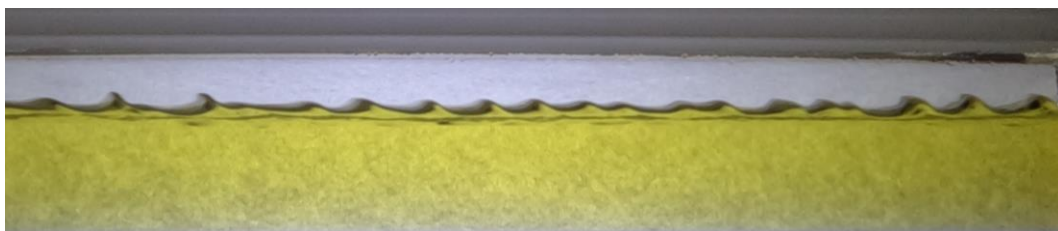


Figure 5. Wavy stratified flow pattern observed ($U_{sl} = 0.1$ m/s, $U_{sg} = 0.5$ m/s).

Furthermore, the algorithm described in the methodology to process differential pressure signals was successfully implemented for eighteen experimental points. The results are presented in Figures 6, 7 and 8 to the P1, P8 and P12,

respectively. Here, only some graphs will be shown, due to the extension of the experimental matrix. However, the global results are presented in Tables 4 and 5 for the mean and variance estimators.

According to the Figure 6, the local mean μ_k calculated for five intervals (20 seg) of the signals remains constant when it compared to the global mean μ ; in the other case, the local variance σ_k^2 varies very little when it compared to the global variance σ^2 . The same behavior is observed for the points P8 and P12, even for the local and the global parameters chosen for the signal analysis. Also, when the superficial velocities of the phases are increased, there is an increase in the oscillation magnitude in the pressure drop, in other words, there is an increase in the variance of the signals, but it is still constant when observed as a local variable; in addition, the autocorrelation function (fig 6.B, 7.B and 8C) were calculated showing that it falls quickly in the 100 first lags, consequently the observations of the pressure drop time series at this lags are the most relevant and contains the most relevant information about the process indicating some repetitive components within it, additionally, the lags that lie within the 95% (gray line) and 99% (dashed gray line) confidence intervals indicate that they are realizations with less relevant information about the process, i.e. they do not affect the behavior of an autoregressive prediction model for the pressure gradient. Therefore, all the signals have a constant tendency with no seasonality component (Moretin & Toloi, 2006), also, the cycle of each time series of rising and falling pressure drops along the constant trend, are repetitive over the entire time interval for all signals studied, verifying the hypotheses that the pressure drop signals corresponds to a stationary process.

According to figure 6C, 7C and 8C, the lag plots shows a large number of points in the pressure gradient series along the main diagonal with a certain spread, this spread indicates the degree of correlation between values in the series indicating the degree of randomness of the process, in this case, the process is not random and can be represented using autoregressive models, or simply a linear model if there is a need to forecast future values. This behavior is repeated for all the experimental points collected, only by varying the operating conditions, which consequently vary the degree of correlation in the time series, but without ceasing to be a stationary process.

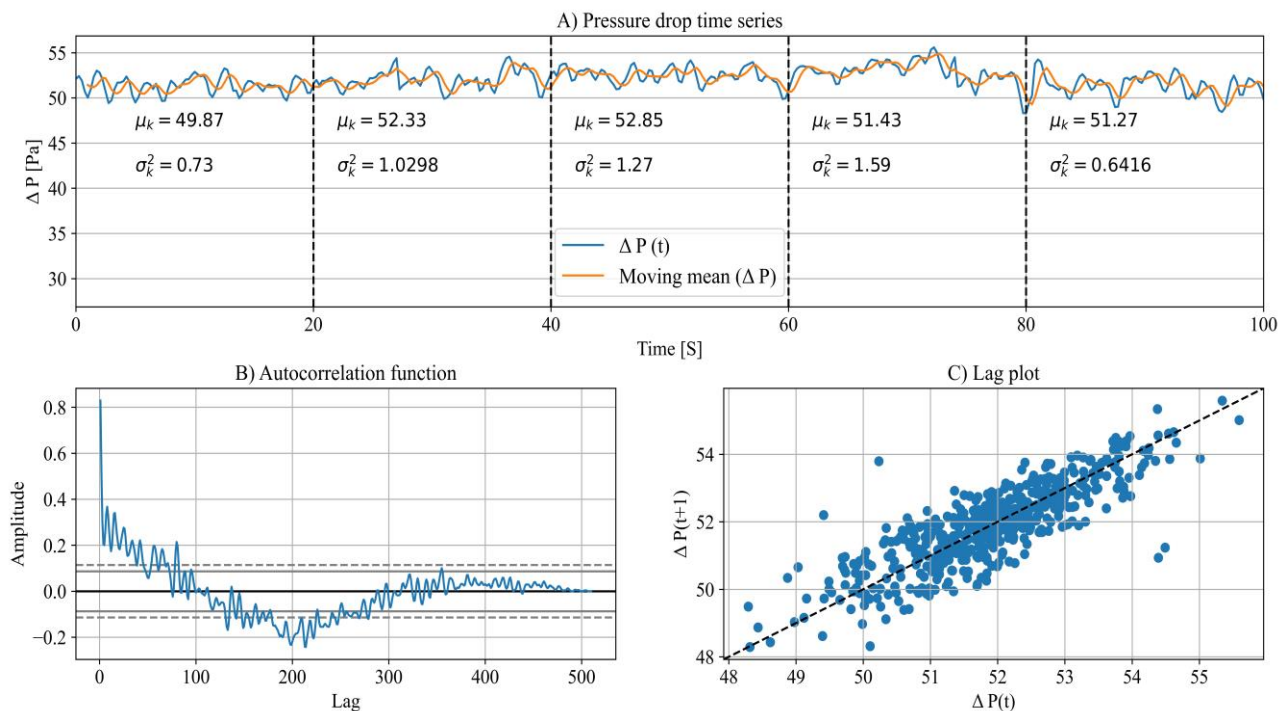


Figure 6. Mean, variance, autocorrelation, and lag analysis for P1($U_{sl} = 0.02$ m/s, $U_{sg} = 0.05$ m/s).

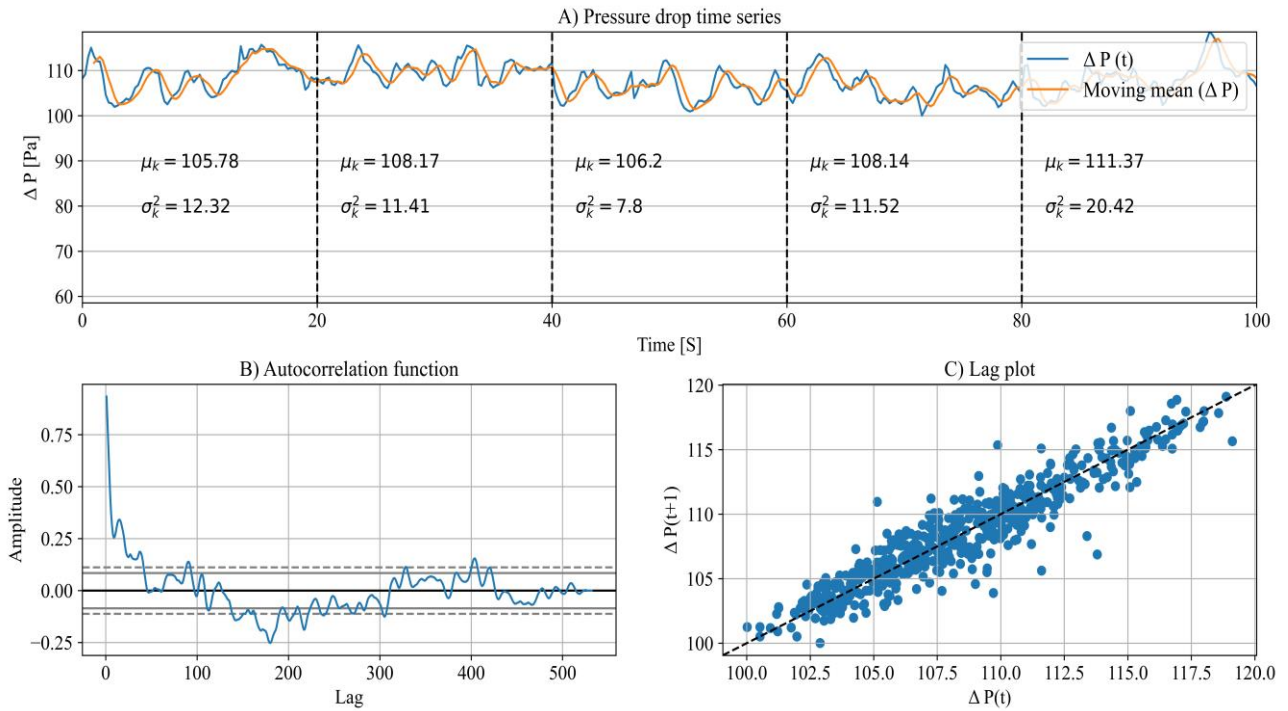


Figure 7. Mean, variance, autocorrelation, and lag analysis for P8 ($U_{sl} = 0.1$ m/s, $U_{sg} = 0.2$ m/s).

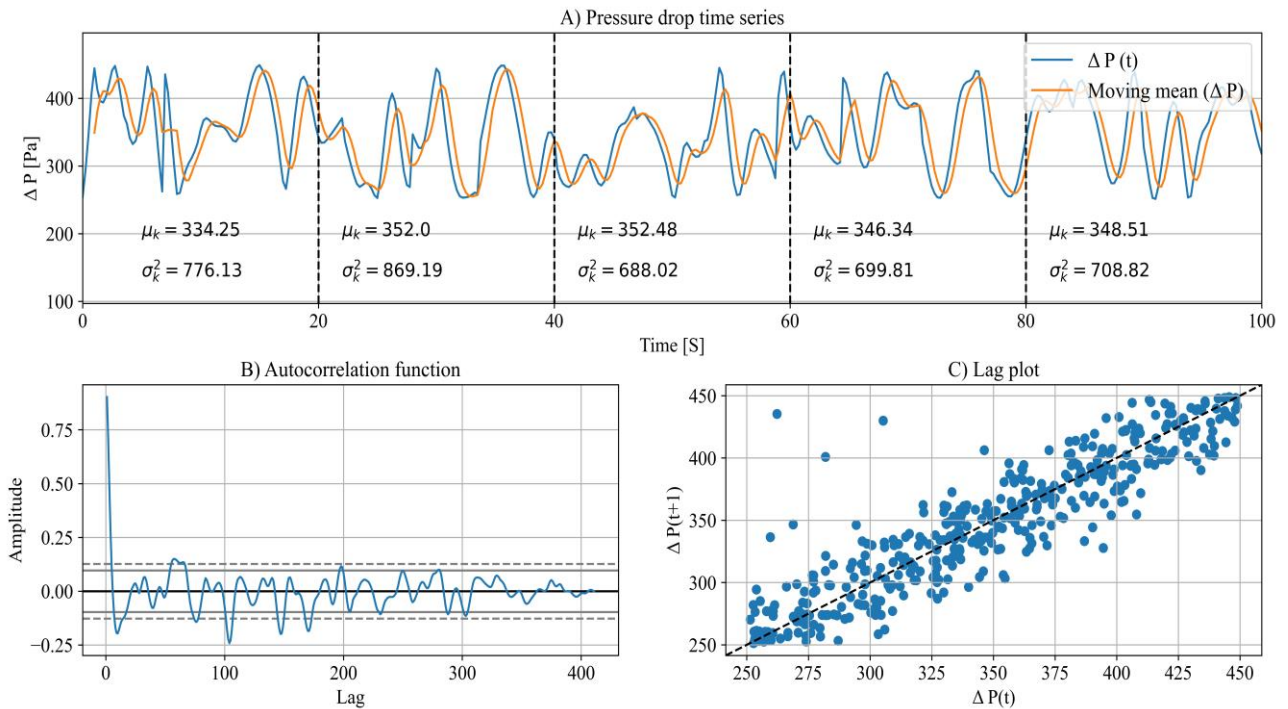


Figure 8. Mean, variance, autocorrelation, and lag analysis for P12 ($U_{sl} = 0.5$ m/s, $U_{sg} = 0.1$ m/s).

In addition, based on Tables 4 and 5, it is observed that for all experimental points and for all time intervals chosen to analyze, both the local and the global mean and variance, can be considered constant. Hence, based on this information, the pressure drops of the oil-SF₆ flow patterns studied.

Table 4. Global and local means of the pressure drop signals collected.

Point	μ [x(n Δ)]	Interval 1	Interval 2	Interval 3	Interval 4	Interval 5
P1	51.8609	49.87884	52.33711	52.85894	51.43356	51.27901
P2	46.282	44.96049	47.48122	46.99723	45.0597	45.22621
P3	55.3329	51.93121	55.36206	55.95457	55.64737	54.82892
P4	73.3271	68.13988	73.55585	73.59394	72.39239	73.1087
P5	94.0682	81.00377	93.81855	94.68849	93.79862	94.88217
P6	59.3219	53.90398	58.33691	59.79342	59.8556	58.14452
P7	76.1935	72.87711	74.36828	78.43184	78.9246	75.24718
P8	90.3356	95.61278	93.55693	91.0214	88.21848	81.96317
P9	108.546	105.7819	108.1708	106.2034	108.1431	111.3746
P10	176.91	163.4886	178.8238	177.5857	176.624	176.8909
P11	337.394	328.8887	339.6403	334.062	338.6058	335.6889
P12	349.094	334.258	352.0028	352.4891	346.3489	348.5115
P13	346.74	355.3758	331.5784	331.0326	349.0076	355.8555
P14	318.221	315.0291	330.3967	313.8598	324.8584	289.1133
P15	400.826	371.5156	403.0059	407.8114	404.7106	396.7116
P16	670.515	662.5999	678.0363	679.8435	666.0615	645.9981
P17	2360.63	1996.684	2367.165	2363.358	2330.952	2406.928
P18	2612.15	2480.888	2633.43	2617.519	2582.846	2608.936

Table 5. Global and local variance of the pressure drop signals collected.

Point	σ^2	Interval 1	Interval 2	Interval 3	Interval 4	Interval 5
P1	1.44124	0.730906	1.029825	1.27082	1.591035	0.641681
P2	3.64685	1.041563	1.927375	1.165321	5.007878	4.29274
P3	1.52544	1.53034	1.300015	0.870598	1.280726	1.627839
P4	1.69433	1.733585	1.223241	1.652611	0.94209	1.38298
P5	1.01887	0.589788	1.074734	0.520467	0.710004	0.231535
P6		0.766886	0.867397	0.35785	0.425993	100.3336
P7	88.9853	82.89551	75.93419	81.03054	102.0166	81.96977
P8	167.045	80.51735	147.1966	123.7064	211.6345	143.5935
P9	15.3445	12.32315	11.41921	7.801112	11.52345	20.42605
P10	10.5234	3.765865	14.73376	7.615958	2.663887	13.6458
P11	326.675	333.1603	362.896	258.7783	307.0357	347.6404
P12	755.088	776.1339	869.1987	688.0216	699.8174	708.827
P13	3025.86	2705.008	3499.807	2012.593	3242.435	2747.955
P14	1674.02	1642.44	1257.524	1646.229	1692.95	1005.544
P15	366.777	354.9653	416.473	259.7637	253.4151	370.7897
P16	1584.5	1110.081	1366.77	1434.958	1958.538	1139.417
P17	1397.43	401.3653	763.9376	959.9537	1063.175	317.9025
P18	2226.21	1978.753	1847.361	2153.297	1580.753	2135.383

4. CONCLUSIONS

A total of eighteen experimental data points were obtained from investigations conducted at the Industrial Multiphase Flow Laboratory- LEMI, under controlled and specific conditions, to examine the dynamics of two-phase dense-gas and oil flow in a horizontal position. The experimental data was systematically characterized by identifying three distinct flow patterns, namely, smooth stratified, wavy stratified, and dispersed. The pressure gradient was determined through rigorous calculations, while the void fraction was accurately measured using a gamma ray densitometer installed on a vertical sliding system.

The time-series analysis was successfully applied, and it was seen that for the oil-SF₆ flow patterns studied, the pressure drop of the multiphase flow with no leak condition can be considered as a stationary process with constant tendency, soft cycling, and no seasonality components for those regimes characterizing a stationary process. However, in the presence of leakage, the pressure drop is expected to change its behavior to a linear tendency and fluctuate between different levels of pressure, which results in a non-stationary process.

5. ACKNOWLEDGEMENTS

We would like to thank the Industrial Multiphase Flow Laboratory (LEMI) at the São Carlos School of Engineering (EESC), University of São Paulo (USP), for their assistance with this study.

6. REFERENCES

- Álvarez-Briceño, R., Kanizawa, F. T., Ribatski, G., & de Oliveira, L. P. R. (2023). Experimental estimation of equivalent loads on upward two-phase crossflow in tube bundles via Kalman filtering. *Journal of Fluids and Structures*, 120, 103900. <https://doi.org/10.1016/j.jfluidstructs.2023.103900>
- Blázquez-García, A., Conde, A., Mori, U., & Lozano, J. A. (2021). Water leak detection using self-supervised time series classification. *Information Sciences*, 574, 528–541. <https://doi.org/10.1016/j.ins.2021.06.015>
- Borg, D., Sestito, G. S., & da Silva, M. M. (2021). Machine-learning classification of environmental conditions inside a tank by analyzing radar curves in industrial level measurements. *Flow Measurement and Instrumentation*, 79(February), 101940. <https://doi.org/10.1016/j.flowmeasinst.2021.101940>
- dos Santos Ambrosio, J., Lazzaretti, A. E., Pipa, D. R., & da Silva, M. J. (2022). Two-phase flow pattern classification based on void fraction time series and machine learning. *Flow Measurement and Instrumentation*, 83(December 2020), 102084. <https://doi.org/10.1016/j.flowmeasinst.2021.102084>
- Fiedler, J. (2016). An overview of pipeline detection technologies. In *Asgmt 2016* (pp. 1–9). KROHNE iNC.
- Idachaba, F., & Tomomewo, O. (2023). Surface pipeline leak detection using realtime sensor data analysis. *Journal of Pipeline Science and Engineering*, 3(2), 100108. <https://doi.org/10.1016/j.jpse.2022.100108>
- Marins, M. A., Barros, B. D., Santos, I. H., Barrionuevo, D. C., Vargas, R. E. V., de M. Prego, T., de Lima, A. A., de Campos, M. L. R., da Silva, E. A. B., & Netto, S. L. (2021). Fault detection and classification in oil wells and production/service lines using random forest. *Journal of Petroleum Science and Engineering*, 197(August 2020), 107879. <https://doi.org/10.1016/j.petrol.2020.107879>
- Martins, J. C., & Selegim, P. (2010). Assessment of the Performance of Acoustic and Mass Balance Methods for Leak Detection in Pipelines for Transporting Liquids. *Journal of Fluids Engineering*, 132(1), 0114011–0114018. <https://doi.org/10.1115/1.4000736>
- Moretin, P. A., & Toloi, C. M. C. (2006). *Análise de Séries Temporais* (2 ed). Edgar Blucher.
- Nascimento, R. S. F. do, Barbosa, B. H. G., Vargas, R. E. V., & Santos, I. H. F. dos. (2021). Detecção de anomalias em poços de petróleo surgentes com stacked autoencoders. *Proceedings Do XV Simpósio Brasileiro de Automação Inteligente*, 2049–2056. <https://doi.org/https://doi.org/10.20906/sbai.v1i1.2856>
- Quintino, A. M. (2022). *Phenomenological, heuristic and experimental study of liquid / dense-gas two-phase pipe flow*. São Carlos School of Engineering, University of São Paulo, São Carlos – SP, 2022.
- Sestito, G. S., Turcato, A. C., Dias, A. L., Ferrari, P., & da Silva, M. M. (2022). Versatile unsupervised anomaly detection method for RTE-based networks. *Expert Systems with Applications*, 206(May 2021), 117751. <https://doi.org/10.1016/j.eswa.2022.117751>
- Shao, Y., Li, X., Zhang, T., Chu, S., & Liu, X. (2019). Time-Series-Based Leakage Detection Using Multiple Pressure Sensors in Water Distribution Systems. *Sensors*, 19(14), 3070. <https://doi.org/10.3390/s19143070>
- Shin, K., & Hammond, J. (2008). *Fundamentals of signal processing for sound and vibration* (1st ed.). Wiley.
- Turan, E. M., & Jaschke, J. (2021). Classification of undesirable events in oil well operation. *2021 23rd International Conference on Process Control (PC)*, 157–162. <https://doi.org/10.1109/PC52310.2021.9447527>
- Vargas, R. E. V., Munaro, C. J., Ciarelli, P. M., Medeiros, A. G., Amaral, B. G. do, Barrionuevo, D. C., Araújo, J. C. D. de, Ribeiro, J. L., & Magalhães, L. P. (2019). A realistic and public dataset with rare undesirable real events in oil wells. *Journal of Petroleum Science and Engineering*, 181(February), 106223. <https://doi.org/10.1016/j.petrol.2019.106223>

- Vieira, Saon C., Fabro, A. T., Rodrigues, R. L. P., da Silva, M. J., Morales, R. E., & Castro, M. S. (2023). A two-state Markov chain model for slug flow in horizontal ducts. *Flow Measurement and Instrumentation*, 90(February), 102335. <https://doi.org/10.1016/j.flowmeasinst.2023.102335>
- Vieira, Saon Crispim, van der Geest, C., Fabro, A. T., Castro, M. S. de, & Bannwart, A. C. (2021). Intermittent slug flow identification and characterization from pressure signature. *Mechanical Systems and Signal Processing*, 148, 107148. <https://doi.org/10.1016/j.ymssp.2020.107148>

7. RESPONSIBILITY NOTICE

Carlos M. Ruiz-Diaz, C. E. Alvarez-Pacheco, Castro-B. Johann E., M. da Silva Carr, and Oscar M. H. Rodriguez are the only responsible for the printed material included in this paper.